Calculations for electron transitions on a three-dimensional lattice in relativistic heavy-ion collisions

Oliver Busic, Norbert Grün, and Werner Scheid

Institut für Theoretische Physik der Justus-Liebig-Universität, Giessen, Germany

In order to calculate the cross section for electron-positron pair production with capture of the electron into the K shell of the target in relativistic scattering of heavy nuclei, we apply the semiclassical method and solve the time-dependent Dirac equation in time-reversal symmetry, starting with a $1s_{1/2}$ state at the target. The solution is carried out numerically on a three-dimensional lattice in coordinate space. Cross sections for excitation, ionization, electron transfer, and pair production with capture are obtained for collisions of $U^{92+}(\gamma=1.5)$, $Au^{79+}(\gamma=2)$, and $U^{92+}(\gamma=10\,000)$ on $U^{91+}(1s_{1/2})$ and U^{92+}, where γ is the Lorentz factor, and compared with experimental data and other theoretical results.

I. INTRODUCTION

The process of pair production with capture, also called bound-free pair production, has been of great interest in the recent years [1]. Because this process constitutes the dominant electron capture mechanism for higher energies in heavy ion collisions, it plays an important role in ultrarelativistic heavy ion colliders where it causes the loss of accelerated nuclei and limits the lifetime of the beams [2]. First measurements for bound-free pair production were performed by Belkacem *et al.* [3] in 1993 and further experimental investigations on its dependence on energy and nuclear charges were published in the following years [4–6].

From the theoretical point of view, a description of pair production with capture also includes the processes of excitation, ionization and charge exchange if one considers the time-reversal symmetry. The time-reverse process starts with a bound electron state at the target and evolves according to the time-dependent Dirac equation under the influence of the projectile potential. Results for pair production with capture were first obtained by Becker *et al.* [7] in time-dependent perturbation theory for the scattering on an $^{92+}$U-target with a projectile energy up to 100 GeV/nucleon. Eichler [8] considered the pair production as a charge transfer process from the negative target continuum to the bound projectile state using the OBK approximation.

The perturbation theory fails for the case of high charges of the heavy ions and at small impact parameters. A strong nonperturbative enhancement was found by Strayer *et al.* [9] for muon pair production with capture by solving the Dirac equation on a lattice with a three-dimensional spline collocation method. Similar effects were observed in nonperturbative calculations for relativistic energies of the heavy ions by Rumrich *et al.* [10] using a one-center coupled channel method and, for example by Gail *et al.* [11], with one- and two-center coupled channel calculations.

For high energetic collisions, Baltz *et al.* [12] obtained the cross section for bound-free pair production in the form $\sigma = A \ln \gamma + B$, where γ is the Lorentz factor of the projectile and A and B are constants. For Pb^{82+}-Pb^{82+} collisions at energies of the Brookhaven Relativistic Heavy Ion Collider

(RHIC), Baltz *et al.* [13] found only a small nonperturbative enhancement of a few percent.

In our group only two-dimensional grid solutions of the Dirac equation for zero impact parameter [14,15] were considered up to now. Here we present a new investigation for pair production with capture where we solve the time-dependent Dirac equation in coordinate space on a three-dimensional lattice. It should be mentioned that three-dimensional calculations with the spline-collocation method in coordinate space were already done by Strayer *et al.* [9] and Wells *et al.* [16–18] for muon pair production with capture in heavy ion collisions. Also, three-dimensional lattice calculations in momentum space were carried out by Momberger *et al.* [19] for Au^{79+}+U^{91+} collisions at low and medium relativistic energies, mostly for zero impact parameter.

The aim of this paper is to give the methods to solve a time-dependent two-center Dirac equation in three spatial dimensions numerically. Starting with a $1s_{1/2}$ state around the target ion we calculate the wave function and extract the probabilities for excitation, ionization, transfer and electron-positron pair production with capture of the electron into the K shell of target after the collision. Then we compare the results with experimental data and other theories as far as possible. We find serious difficulties to interpret the numerically gained wave functions in terms of the calculated probabilities for the created electron-positron pairs. The reason for these difficulties lies in our unknowing about the exact positron states in the field of two moving ions.

In Sec. II we review the semiclassical theory of pair production with capture. The procedure for solving the time-dependent Dirac equation on a three-dimensional grid is given in Sec. III. In Sec. IV we present and discuss the results of our calculations for U^{92+}(466 MeV/nucleon) +U^{91+}, Au^{79+}(930 MeV/nucleon)+U^{91+} and for the ultrarelativistic scattering of U^{92+} on U^{91+}.

II. THEORY

We consider the process of electron-positron pair production as an excitation of an electron of the fully occupied

negative continuum into a bound or positive continuum state (see Ref. [1]). The wave functions of these states fulfill the time-dependent Dirac equation with the following Hamiltonian written in the target system:

$$H = H_{0T} + W_P, \tag{1}$$

where

$$H_{0T} = c\boldsymbol{\alpha}\mathbf{p} + \beta mc^2 - eV_T, \tag{2}$$

$$W_P = ec\boldsymbol{\alpha}\mathbf{A}_P - eV_P \tag{3}$$

with

$$V_T = \frac{1}{4\pi\varepsilon_0} \frac{Z_T e}{\sqrt{x^2 + y^2 + z^2}}, \tag{4}$$

$$V_P = \frac{\gamma}{4\pi\varepsilon_0} \frac{Z_P e}{\sqrt{x^2 + (y - b)^2 + \gamma^2(z - v_P t)^2}}, \tag{5}$$

$$\mathbf{A}_P = \frac{\beta}{c} V_P \mathbf{e}_z. \tag{6}$$

Here, we apply the semiclassical approximation and treat the nuclei as point charges with charge numbers Z_P and Z_T, respectively, moving classically on straight lines with a constant velocity v_P of the projectile in the target system and an impact parameter $b[\beta = v_P/c, \gamma = (1 - \beta^2)^{-1/2}]$. Further, H_{0T} is the unperturbed target Hamiltonian with analytic Coulomb-Dirac eigenfunctions $\phi_{\lambda\pm}$,

$$H_{0T}\phi_{\lambda\pm}(\mathbf{r}) = E_{\lambda\pm}\phi_{\lambda\pm}(\mathbf{r}). \tag{7}$$

The index $\lambda+$ denotes a state of the positive continuum or a bound state and $\lambda-$ a state of the negative continuum. These states are used to fix the initial conditions of the solutions of the time-dependent Dirac equation with the Hamiltonian (1). Writing this equation as

$$H\Psi_{\lambda\pm}(\mathbf{r},t) = i\hbar\frac{\partial}{\partial t}\Psi_{\lambda\pm}(\mathbf{r},t), \tag{8}$$

we demand as initial condition for $t \to -\infty$,

$$\lim_{t \to -\infty} \Psi_{\lambda\pm}(\mathbf{r},t) = \phi_{\lambda\pm}(\mathbf{r})\exp(-iE_{\lambda\pm}t/\hbar). \tag{9}$$

Then, by using a field-theoretical approach the expectation values of the numbers of created electrons and positrons per state can be calculated as

$$N^{e^-}_{\lambda+} = \sum_{\mu-} |\langle \phi_{\lambda+}|\Psi_{\mu-}(\mathbf{r},t \to \infty)\rangle|^2, \tag{10}$$

$$N^{e^+}_{\lambda-} = \sum_{\mu+} |\langle \phi_{\lambda-}|\Psi_{\mu+}(\mathbf{r},t \to \infty)\rangle|^2. \tag{11}$$

Equation (10) [and equivalently (11)] can be rewritten by using the time-reversal symmetry,

$$N^{e^-}_{\lambda+} = \sum_{\mu-} |\langle \phi_{\mu-}|\Psi_{\lambda+}(\mathbf{r},t \to \infty)\rangle|^2. \tag{12}$$

The advantage of Eq. (12) compared to Eq. (10) is that only one single time evolution must be carried out. For example, if one is interested in the electron-positron creation with capture of the electron into a bound state $\lambda+$, one must calculate the time evolution of $\Psi_{\lambda+}(\mathbf{r},t)$ with Eq. (8). In the following we only consider the time evolution of the $1s_{1/2}$ state which yields information on the electron-positron pair creation with capture of the electron into the $1s_{1/2}$ state.

The expectation values (10)–(12) of numbers of created electrons and positrons are interpreted as probabilities for the creation of the corresponding particles. Cross sections are obtained by integrating the probabilities multiplied with the factor $2\pi b$ over the impact parameter.

III. DESCRIPTION ON THE LATTICE

A. Discretized Dirac equation

We introduce an equidistant three-dimensional Cartesian grid on which we define finite elements with respect to each Cartesian coordinate. The corresponding basis functions on the grid are written as products of the form $\varphi_i(x)\varphi_j(y)\varphi_k(z)$. The indices (i,j,k) denote a grid point $P_{ijk} = (x_i = ih, y_j = jh, z_k = kh)$ with $i(j,k) = 1,2,3,\ldots,N_x(N_y,N_z)$ where h is the grid width. The functions $\varphi_i(x)\varphi_j(y)\varphi_k(z)$ are real, extended over a small number of elements and symmetric around their middle points P_{ijk}. They are chosen (see Sec. III C) to fulfill the equations on the grid points

$$\varphi_i(x_{i'}) = \delta_{ii'}, \quad \varphi_j(y_{j'}) = \delta_{jj'}, \quad \varphi_k(z_{k'}) = \delta_{kk'}. \tag{13}$$

This means that, for example, the function $\varphi_i(x)$ is one at its middle point $x = x_i$ and has zeroes at the other grid points.

Then we choose an ansatz for the time-dependent solution $\Psi(\mathbf{r},t)$ of the Dirac equation (8) in terms of these basis functions, which are assumed as real. By omitting the signature $\lambda\pm$ we write

$$\Psi(\mathbf{r},t) = \sum_{i,j,k} \varphi_i(x)\varphi_j(y)\varphi_k(z) \begin{pmatrix} a^1_{ijk}(t) \\ a^2_{ijk}(t) \\ a^3_{ijk}(t) \\ a^4_{ijk}(t) \end{pmatrix}. \tag{14}$$

Inserting this expansion into (8) and projecting with the real basis functions, we obtain a matrix equation for the time-dependent expansion coefficients $a^\nu_{ijk}(t)$ which are collected in a spinor $\mathbf{a}(t)$:

$$i\hbar\mathbf{M}\frac{d}{dt}\mathbf{a}(t) = \mathbf{H}\mathbf{a}(t) \tag{15}$$

with

$$\mathbf{a}(t) = \begin{pmatrix} a_{111}^1(t) \\ a_{111}^2(t) \\ a_{111}^3(t) \\ a_{111}^4(t) \\ a_{112}^1(t) \\ \vdots \\ a_{N_x N_y N_z}^4(t) \end{pmatrix} \qquad (16)$$

and

$$\mathbf{M} = \mathbf{M}^x \otimes \mathbf{M}^y \otimes \mathbf{M}^z \otimes \mathbf{I}^4, \qquad (17)$$

$$\mathbf{H} = c\mathbf{K}^x \otimes \mathbf{M}^y \otimes \mathbf{M}^z \otimes \alpha_x + c\mathbf{M}^x \otimes \mathbf{K}^y \otimes \mathbf{M}^z \otimes \alpha_y$$
$$+ c\mathbf{M}^x \otimes \mathbf{M}^y \otimes \mathbf{K}^z \otimes \alpha_z + mc^2\mathbf{M}^x \otimes \mathbf{M}^y \otimes \mathbf{M}^z \otimes \beta$$
$$- e(\mathbf{V}_T + \mathbf{V}_P) \otimes \mathbf{I}^4 + e(v_P/c)\mathbf{V}_P \otimes \alpha_z. \qquad (18)$$

The sign $\otimes$ means matrix multiplication. The matrices $\mathbf{M}^{x,y,z}$ are the overlap matrices and the matrices $\mathbf{K}^{x,y,z}$ the matrices of the momentum operator. For example, we have the elements

$$M_{ii'}^x = \int \varphi_i(x)\varphi_{i'}(x)dx, \quad K_{ii'}^x = -i\hbar \int \varphi_i(x)\frac{d}{dx}\varphi_{i'}(x)dx. \qquad (19)$$

The matrix elements of the scalar potentials $\mathbf{V} = \mathbf{V}_T$ or $\mathbf{V}_P$ are given by

$$V_{(ijk),(i'j'k')}$$
$$= \int \varphi_i(x)\varphi_j(y)\varphi_k(z)V(\mathbf{r},t)\varphi_{i'}(x)\varphi_{j'}(y)\varphi_{k'}(z)dx\,dy\,dz. \qquad (20)$$

Because these matrix elements are only nonzero for neighboring finite elements, we simplify the potential matrix elements by the approximation

$$V_{(ijk),(i'j'k')} = \tfrac{1}{2}(V(x_i,y_j,z_k,t) + V(x_{i'},y_{j'},z_{k'},t))M_{ii'}^x M_{jj'}^y M_{kk'}^z. \qquad (21)$$

This potential matrix is Hermitean.

B. Time evolution of the discretized Dirac equation

The formal solution of Eq. (15) for a small time interval Δt is given by

$$\mathbf{a}(t + \Delta t) = \exp(-i\mathbf{M}^{-1}\mathbf{H}\Delta t/\hbar)\mathbf{a}(t), \qquad (22)$$

where we assume $\mathbf{H}$ to be constant during the time interval Δt. The exponential operator is expanded in power series of Δt up to the order n and calculated as follows:

$$\exp(-x) = \left(1 - x\left\{1 - \frac{x}{2}\left[1 - \frac{x}{3}\left(\cdots - \frac{x}{n}\cdots\right)\right]\right\}\right). \qquad (23)$$

A high numerical accuracy could be reached.

C. Requirements for the basis functions

The basis functions, fulfilling Eq. (13), are chosen so that the eigenvalues and eigenfunctions of the momentum operator are reproduced in an optimum manner. The eigenvalue equation of the momentum operator is

$$\frac{\hbar}{i}\frac{d}{dx}f(x) = \lambda f(x). \qquad (24)$$

If the function $f(x)$ is expanded with real basis functions,

$$f(x) = \sum_{i=1}^N a_i\varphi_i(x),$$

Eq. (24) leads to a matrix equation for the coefficients a_i,

$$\sum_j K_{ij}a_j = \lambda \sum_j M_{ij}a_j \qquad (25)$$

with

$$M_{ij} = \int \varphi_i(x)\varphi_j(x)dx,$$

$$K_{ij} = -i\hbar \int \varphi_i(x)\frac{d}{dx}\varphi_j(x)dx.$$

We require for the basis functions $\varphi_i(x)$ that (i) they are real, (ii) they are defined on an equidistant grid with the distance h between two neighboring grid points, (iii) they fulfill Eq. (13), (iv) they are symmetric with respect to the grid points $x = ih$, and (v) they are extended over a small number of elements in the interval $(i - [n+1]/2)h \leqslant x \leqslant (i + [n+1]/2)h$ with $n = 1, 2, \ldots$. Then we can introduce the following replacements:

$$M_{i,i\pm s} = hm_s \text{ with } s = 0, 1, \ldots, n,$$

$$K_{i,i\pm s} = \mp i\hbar d_s \text{ with } s = 1, 2, \ldots, n, \qquad (26)$$

where m_s and d_s are real quantities. With the ansatz $a_j = \exp(ikjh)$ with $-\pi \leqslant kh \leqslant \pi$ one can solve the eigenvalue problem (25) (see Ref. [20,21]):

$$\lambda(k) = \frac{2\hbar}{h}\frac{\sum_{s=1}^n d_s \sin(ksh)}{m_0 + 2\sum_{s=1}^n m_s \cos(ksh)}. \qquad (27)$$

In order to confine the freedom in the choices of the basis functions, we demand that $\lambda(k) = \hbar k$ up to the order of k^{n+2}. This leads to the conditions for $n = 1$,

$$d_1 = \tfrac{1}{2}(m_0 + 2m_1), \qquad (28)$$

for $n = 2$,

$$d_1 + 2d_2 = \tfrac{1}{2}m_0 + m_1 + m_2,$$

$$d_1 + 8d_2 = 3(m_1 + 4m_2), \qquad (29)$$

and for $n = 3$,

$$d_1 + 2d_2 + 3d_3 = \tfrac{1}{2}m_0 + m_1 + m_2 + m_3,$$

$$d_1 + 8d_2 + 27d_3 = 3(m_1 + 4m_2 + 9m_3), \qquad (30)$$

$$d_1 + 32d_2 + 243d_3 = 5(m_1 + 16m_2 + 81m_3).$$

Linear tent functions $\varphi_i(x) = 1 - |(x/h) - i|$ for $i-1 \leqslant x/h \leqslant i + 1$ and 0 otherwise belong to $n=1$. In this case we have $m_0 = 2/3$, $m_1 = 1/6$, $d_1 = 1/2$ and condition (28) is fulfilled.

The procedure of solving the time-dependent coupled equation (15) simplifies if we additionally require the orthonormalization of the basis functions. This means

$$m_s = \delta_{s0}. \qquad (31)$$

With this condition we obtain from Eqs. (28)–(30),

$$n=1, \quad d_1 = \tfrac{1}{2}; \quad n=2, \quad d_1 = \tfrac{2}{3}, \quad d_2 = -\tfrac{1}{12};$$

$$n=3, \quad d_1 = \tfrac{3}{4}, \quad d_2 = -\tfrac{3}{20}, \quad d_3 = \tfrac{1}{60}. \qquad (32)$$

The coefficients d_s are the coefficients of approximate differential formulas derived from interpolation formulas and may be taken for higher values of n from the literature [22].

The functions $\varphi_i(x)$ fulfilling all demanded requirements are usually complicated functions [23]. However, their explicit form is not needed in solving Eq. (15) since we replaced the interaction matrix (20) by mean values at the grid points. Also the projection of the calculated final wave function on given analytical wave functions can be done on the same grid by only using the values at the grid points according to Eq. (13). Therefore, we could use Eqs. (31) and (32) in our calculations without an explicit knowledge of the functions $\varphi_i(x)$.

D. Initial solution for the $1s_{1/2}$ state on the lattice

As stated above, we only consider the time evolution of an initial $1s_{1/2}$ state. In order to construct an equivalent spinor for this state on the lattice, we treat the following eigenvalue problem on the grid:

$$\mathbf{M}^{-1}\mathbf{H}_0\mathbf{a} = E\mathbf{a}, \qquad (33)$$

where

$$\mathbf{H}_0 = \lim_{t \to -\infty} \mathbf{H}(t) = \mathbf{H}(V_P = 0).$$

We search for the lowest eigenvalue $E = E_0$ of the bound states. This is done by a two-step method. In the first step we calculate the eigenvalue $E_{\max}$ with the largest absolute value by the iteration method of von Mises,

$$\mathbf{a}_i = \mathbf{M}^{-1}\mathbf{H}_0\mathbf{a}_{i-1}/N_{i-1}, \qquad (34)$$

with

$$\lim_{i \to \infty} \mathbf{a}_i = \tilde{\mathbf{a}} \text{ and } \mathbf{M}^{-1}\mathbf{H}_0\tilde{\mathbf{a}} = E_{\max}\tilde{\mathbf{a}},$$

where N_{i-1} is a normalization constant. In the second step we again use the method of von Mises and calculate the largest eigenvalue $\epsilon_{\max}^2$ of the eigenvalue equation

$$[E_{\max}^2 - (\mathbf{M}^{-1}\mathbf{H}_0)^2]\mathbf{a} = \epsilon^2\mathbf{a}. \qquad (35)$$
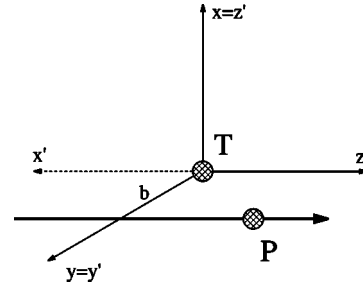

FIG. 1. Coordinate systems (x,y,z) and (x',y',z'). The trajectory is shown by a thick line in a distance b parallel to the z axis. The target nucleus is at the coordinate origin and the projectile nucleus moves on the trajectory.

Since the energy E_0 of the $1s_{1/2}$ state up to uranium is the smallest positive eigenvalue of $\mathbf{M}^{-1}\mathbf{H}_0$ and no eigenvalues exist in the interval $(-mc^2, 0)$, the eigenvalue $E = E_0$ maximizes the function $\epsilon^2 = E_{\max}^2 - E^2$. Therefore, the spinor $\mathbf{a}_{\max} = \mathbf{a}_0$ to the eigenvalue $\epsilon_{\max}^2 = E_{\max}^2 - E_0^2$ is simultaneously eigenspinor to the equation $(\mathbf{M}^{-1}\mathbf{H}_0)^2\mathbf{a}_0 = E_0^2\mathbf{a}_0$.

The eigenvalue E_0 and eigenspinor $\mathbf{a}_0$ obtained by the method described above are the lattice replacements for the analytical $1s_{1/2}$ state. According to the Coulomb-Dirac equation the $1s_{1/2}$ energy for $Z=92$ is 378.4 keV. With the above method we get 379.9 keV for the energy and a value of 0.997 for the absolute square of the overlap between the analytic and lattice-type $1s_{1/2}$ spinor. These results were reached with a cubic grid with a length of the sides of 10 000 fm and 216 grid points in each Cartesian direction of space.

E. Symmetry relations

As indicated in Eqs. (5) and (6), the projectile moves along a straight line described by the vector $\mathbf{R} = (0, b, v_P t)$. In order to make use of symmetry relations, it is of some advantage to quantize the spinors of the initial wave function in the x direction, which is the z' axis of a dashed coordinate system defined as (see Fig. 1)

$$z' = x, \quad x' = -z, \quad y' = y. \qquad (36)$$

1. Reflection on the plane $x=0$

The Dirac-Hamiltonian (1) is invariant under the action of the product of the parity operator P_x in the x coordinate and a (4×4)-matrix S_x for the spin,

$$S_x P_x H(p_x, p_y, p_z, x, y, z, t) = S_x H(-p_x, p_y, p_z, -x, y, z, t) P_x$$
$$= H(p_x, p_y, p_z, x, y, z, t) S_x P_x \qquad (37)$$

with

$$S_x = \begin{pmatrix} \sigma_x & 0 \\ 0 & -\sigma_x \end{pmatrix} \qquad (38)$$

and

$$\{\alpha_x, S_x\} = [\alpha_y, S_x] = [\alpha_z, S_x] = [\beta, S_x] = 0. \qquad (39)$$

Eigenfunctions of the operator $S_x P_x$ have the eigenvalues ± 1. Therefore, if the initial wave function is an eigenfunction of

$S_x P_x$, it remains for all times with the property

$$\Psi(-x,y,z,t) = \pm S_x \Psi(x,y,z,t). \tag{40}$$

Bound Coulomb-Dirac eigenfunctions $\phi_{\kappa m}$, quantized in the x direction, are eigenfunctions of $S_x P_x$,

$$S_x P_x \phi_{\kappa m} = (-1)^{\ell_A + m - 1/2} \phi_{\kappa m}, \tag{41}$$

where ℓ_A is the ℓ value of the large component. Since initially we start with the $1s_{1/2}$ state, we can use the symmetry relation (wave function quantized in the x direction),

$$\Psi_{\kappa=-1,m}(-x,y,z,t) = (-1)^{m-1/2} S_x \Psi_{\kappa=-1,m}(x,y,z,t). \tag{42}$$

This means that the wave function needs only to be calculated for $x \geq 0$.

2. Impact parameter symmetry

The Dirac-Hamiltonian (1) is invariant under the action of the product of three operators

$$\begin{aligned} S_y P_y P_b H(p_x,p_y,p_z,x,y,z,t,b) &= S_y H(p_x,-p_y,p_z,x,-y,z,t, \\ &\quad -b) P_y P_b \\ &= H(p_x,p_y,p_z,x,y,z,t,b) S_y P_y P_b. \end{aligned} \tag{43}$$

Here, P_b replaces b by $-b$, P_y is the parity operator in the y coordinate and

$$S_y = \begin{pmatrix} \sigma_y & 0 \\ 0 & -\sigma_y \end{pmatrix} \tag{44}$$

with

$$\{\alpha_y, S_y\} = [\alpha_x, S_y] = [\alpha_z, S_y] = [\beta, S_y] = 0. \tag{45}$$

Eigenfunctions of the operator $S_y P_y$ have the eigenvalues ± 1. Coulomb-Dirac eigenfunctions $\phi_{\kappa m}$, quantized in the x direction, which is the z' direction in the dashed coordinate system [see Eq. (36)], have the property under the action of $S_y P_y$,

$$S_y P_y \phi_{\kappa m}(\mathbf{r}) = i(-1)^{m+1/2} \frac{\kappa}{|\kappa|} \phi_{\kappa-m}(\mathbf{r}). \tag{46}$$

This relation can be used to obtain the function $\Psi_{\kappa-m}(\mathbf{r},t,b)$ from the function $\Psi_{\kappa m}(\mathbf{r},t,-b)$, which solves the time-dependent Dirac equation with the Hamiltonian $H(\mathbf{p},\mathbf{r},t,-b)$, i.e., with a negative impact parameter $-b$. The connection is

$$\Psi_{\kappa-m}(\mathbf{r},t,b) = -i(-1)^{m+1/2} \frac{\kappa}{|\kappa|} S_y P_y \Psi_{\kappa m}(\mathbf{r},t,-b) \tag{47}$$

with

$$\lim_{t \to -\infty} \Psi_{\kappa m}(\mathbf{r},t,-b) = \phi_{\kappa m}(\mathbf{r}) \exp(-iE_\kappa t/\hbar).$$

Since we start our time development with the $1s_{1/2}$ state, we only need to calculate the wave function with $m=m_{j_x} = 1/2$, but for positive and negative impact parameters. The cross section for pair production with capture of the electron into the K shell can then be written as

$$\begin{aligned} \sigma_{pp} &= \int_0^\infty 2\pi b \, db \sum_{\mu-} [|\langle \phi_{\mu-}|\Psi_{1s_{1/2},1/2}(\mathbf{r},t\to\infty,b)\rangle|^2 \\ &\quad + |\langle \phi_{\mu-}|\Psi_{1s_{1/2},-1/2}(\mathbf{r},t\to\infty,b)\rangle|^2] \\ &= \int_{-\infty}^\infty 2\pi|b|db \sum_{\mu-} |\langle \phi_{\mu-}|\Psi_{1s_{1/2},1/2}(\mathbf{r},t\to\infty,b)\rangle|^2. \end{aligned} \tag{48}$$

In a similar way the excitation, ionization, and transfer cross sections for a target electron in the K shell are calculated, where a factor $1/2$ must be included by assuming an unpolarized hydrogenlike target ion.

F. Gauge transformation

In order to have better asymptotic solutions, we follow Eichler [24] and apply a phase transformation to the spinor $\Psi(\mathbf{r},t)$ by the ansatz

$$\Psi(\mathbf{r},t) = \exp[-i\nu_P \ln(R' - \nu_P t')]\Psi'(\mathbf{r},t), \tag{49}$$

where

$$\nu_P = \frac{Z_P e^2}{4\pi\varepsilon_0 \hbar \nu_P}, \quad R' = \sqrt{b^2 + \nu_P^2 t'^2}, \quad t' = \gamma\left(t - \frac{\nu_P z}{c^2}\right). \tag{50}$$

This leads to a Dirac equation for $\Psi'(\mathbf{r},t)$ with the modified projectile potentials

$$V_P' = \frac{\gamma Z_P e}{4\pi\varepsilon_0}\left(\frac{1}{r_P} - \frac{1}{R'}\right), \quad A_z' = \frac{\beta}{c}V_P',$$

$$r_P = [x^2 + (y-b)^2 + \gamma^2(z-\nu_P t)^2]^{1/2}. \tag{51}$$

These potentials are zero at the coordinate origin for all times, i.e., at the location of the target ion, and fall off faster near the target for large projectile-target distances than the potentials (5) and (6). This behavior has the consequence that the function $\Psi'(\mathbf{r},t)$ approaches its asymptotic values faster than the function $\Psi(\mathbf{r},t)$. For large positive and negative times the phase factor in (49) depends essentially only on time if the coordinate z is restricted to a region around the target ion,

$$\lim_{t \to -\infty} \Psi(\mathbf{r},t) = c_1(t)\Psi'(\mathbf{r},t), \quad |c_1| = 1,$$

$$\lim_{t \to \infty} \Psi(\mathbf{r},t) = c_2(t)\Psi'(\mathbf{r},t), \quad |c_2| = 1.$$

Therefore, we use the bound $1s_{1/2}$-wave function as initial condition for $\Psi'(\mathbf{r},t)$ and the eigensolutions $\phi_{\lambda\pm}$ of Eq. (7) for projection on $\Psi'(\mathbf{r},t)$ since the time-dependent factor $c_2(t)$ drops out from the probabilities after the collision,

$$\lim_{t \to \infty}|\langle \phi_{\mu\pm}|\Psi_{\lambda+}\rangle|^2 = \lim_{t \to \infty}|\langle \phi_{\mu\pm}|\Psi_{\lambda+}'\rangle|^2.$$

The probability on the right-hand side assumes its asymptotic value ($t \to \infty$) at much smaller times than the expression on the left-hand side because Ψ' solves the Dirac

equation with the screened potential (51). In conclusion we can project with the states $\phi_{\mu\pm}$ unperturbed by the projectile instead of the solutions $\exp[-i\nu_P \ln(R'-v_P t')]\phi_{\mu\pm}$ of the asymptotic two-center Dirac equation for an electron near the target, but distant from the projectile. For an extended discussion of this point see Ref. [25].

G. The problem of Fermion doubling

Fermion doubling occurs in numerical formulations of the Dirac equation on lattices when the operators of the first derivative are replaced by difference expressions [26]. The authors of this paper proposed a special method which allows to avoid Fermion doubling by introducing a unitary transformation of the Dirac equation [27]. However, here we take no special method into account to avoid the Fermion doubling besides the condition of the conservation of the norm of the wave function.

For the present numerical solution of the Dirac equation it is difficult to find a dispersion relation since Eq. (15) is time dependent because of the potentials [see Eq. (21)]. In the case of the free Dirac equation [$\mathbf{V}_T$ and $\mathbf{V}_P = 0$ in Eq. (18)] we derive the following dispersion relation by making use of Eq. (25):

$$E^2 = m^2 c^4 + c^2[\lambda^2(k_x) + \lambda^2(k_y) + \lambda^2(k_z)],$$

where $\lambda(k)$ is given in Eq. (27) and k_x, k_y, and k_z are the Cartesian components of the wave number of the free particle. The dispersion relation has the following form for the simplest case ($m_s = \delta_{s0}$, $n = 1$, $d_1 = 1/2$):

$$E^2 = m^2 c^4 + \frac{c^2 \hbar^2}{h^2}[\sin^2(k_x h) + \sin^2(k_y h) + \sin^2(k_z h)],$$

where we assumed an equal grid distance h in all directions. This formula shows the Fermion doubling phenomenon: unphysical waves with small energies $E \approx mc^2$ for maximal wave numbers $k_x, k_y, k_z = \pi/h$. Therefore, contributions in the numerical solution of the Dirac equation with momenta in the order of $\hbar\pi/h$ and energies around mc^2 could appear.

In our treatment these unphysical states negligibly contribute to the calculated reaction probabilities for the following reasons: The numerically obtained wave functions are projected with analytical wave functions which follow the usual physical relation between momentum and energy, e.g., $E = \pm(m^2 c^4 + c^2 \hbar^2 \mathbf{k}^2)^{1/2}$ for free particles. The analytical wave functions have small momenta for small energies and *vice versa*. For example, if we choose k_x, k_y, $k_z = \pi/h$ with $h = 100$ fm, we calculate $E = 21 mc^2$ for a free particle. We found that the projection with analytical wave functions, possessing the same large wave numbers as the energetically lowest unphysical states with an energy near mc^2, yielded negligible contributions to our probabilities. Therefore, the contribution of the unphysical states in the numerical wave function is small. Projection with analytical wave functions at low energies have small momenta and cannot pick up noticeable contributions from the unphysical states with high momenta. We conclude that mainly the states with momenta around $p = \hbar\pi/(2h)$ may be the most disturbing ones which need further investigations. However, these intermediate momenta and energies also play no essential role in our final results since the main contributions to the probabilities arise from lower energies $|E| \approx 1-2mc^2$ and lower momenta $p < \hbar\pi/(2h) = 3$ MeV/c.

IV. RESULTS

A. U^{92+}(466 MeV/nucleon)+U^{91+} scattering

First we consider the impact of U^{92+} ions on U^{91+} ions at 466 MeV/nucleon. The Lorentz factor of the projectile is $\gamma = 1.5$. At such low energies the probabilities for pair creation are rather small. Therefore, we only discuss the processes of excitation, ionization, and charge transfer of the electron. As unit of length we use 1 fm$= 10^{-15}$ m in the following. The K shell radius of uranium is 575 fm calculated as $a_0/92$ where $a_0 = 0.529 \times 10^{-10}$ m is the Bohr radius. Choosing a total length of the grid in the order of 12 000 fm means lengths of about 20 K shell radii.

The equidistant grid used in this case has an extension in the z direction from -4200 fm to 7150 fm with 118 grid points, in y direction from -6500 fm to 6500 fm with 136 grid points and in x direction from -6500 fm to 0 fm with 68 grid points (the symmetry with respect to the yz plane is used). The range in the z direction is slightly enhanced towards larger values of z in order to have a better description for the electron moving in the direction of the projectile velocity. We use basis functions which are extended over two neighboring elements, which means $n = 1$ (see Sec. III C). We choose the time step $\Delta t = 4.34$ fm/c. For each time step the time evolution operator is expanded up to the seventh order of the Hamiltonian matrix $\mathbf{H}$ [see Eqs. (22) and (23)].

The time evolution starts when the projectile enters the grid at $z = -4200$ fm and ends when the projectile is at $z = 4300$ fm. This means more than 2600 time steps. The start vector is obtained by the von Mises iteration procedure. After we stop the time evolution, we project on bound target states with principal quantum numbers $n \le 7$ to obtain the probabilities for excitation. To calculate the probabilities for ionization, we project on states of the positive continuum with $|\kappa| \le 5$ up to an energy of $4.3mc^2$. For these quantities we can also calculate the probabilities within the first order of perturbation theory by the formula

$$P_{if} = 4\nu_P^2 \left| \langle \phi_f | (1 - \beta\alpha_z) \right.$$
$$\left. \times \exp(iq_0 z) K_0 \left(\frac{q_0}{\gamma} \sqrt{x^2 + (y-b)^2} \right) | \phi_i \rangle \right|^2 \quad (52)$$

with $\nu_P = (Z_P e^2)/(4\pi\epsilon_0 \hbar v_P)$ and $q_0 = (E_f - E_i)/(\hbar v_P)$.

The impact parameter dependent probability for the excitation of the target electron is shown in Fig. 2. For large impact parameters we find a good agreement with the perturbation theory (dashed curve). At small impact parameters, the nonperturbative results are much smaller than the results of the perturbation theory. The nonperturbative results depend on the gauge used in the calculations, whereas the first-order perturbation theory is shown to be independent of the gauge [1,28]. We obtain a total cross section for excitation of
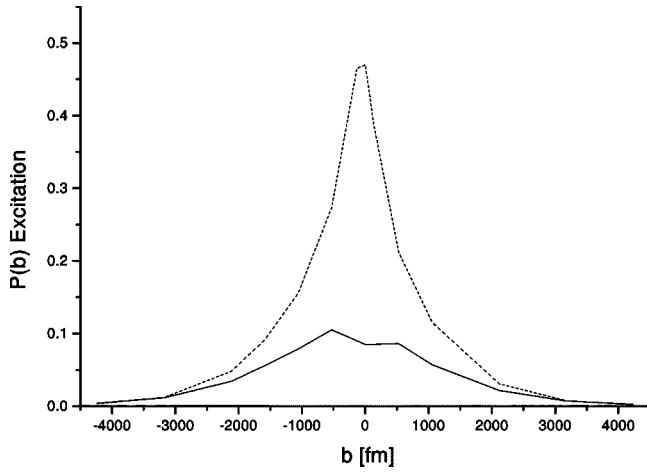
FIG. 2. Probability for excitation of the target electron from the $1s_{1/2}(m_{j_x}=1/2)$ state in the collision of $U^{92+}(\gamma=1.5)$ on U^{91+} as a function of the impact parameter. The full curve is calculated with the lattice method, the dashed curve is the result of the perturbation theory.

$\sigma_{exc}=1.36\times10^4 b$, whereas the perturbation theory yields $2.02\times10^4 b$.

The probability for ionization is shown in Fig. 3. The perturbative results (dashed curve) exceed unity at small impact parameters, whereas the results of the lattice calculations remain smaller than unity (full curve). At larger impact parameters we find good agreement between the results of both methods. The total cross section for ionization is found to be $1.9\times10^4 b$ with the lattice calculation and $2.0\times10^4 b$ with the perturbation method.

To calculate the amplitudes for the electron transfer to the ground state of the projectile, we project on the boosted ground state wave function of the projectile. The transfer probability is depicted in Fig. 4. For the total cross section of transfer we found a value of $1.2\times10^3 b$. The transfer reaction is also clearly visible in the density $|\Psi|^2$. Figure 5 shows the density in the scattering plane at the time $t=4780$ fm/c. The
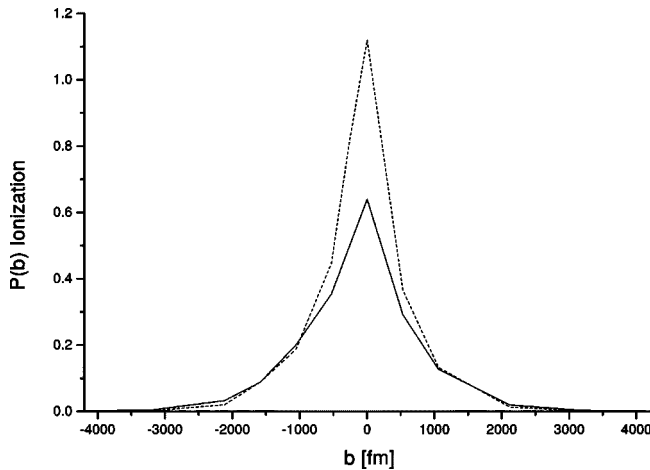

FIG. 3. Probability for ionization of the target electron from the $1s_{1/2}(m_{j_x}=1/2)$ state for the same collision system as in Fig. 2. The notations are the same as in Fig. 2.
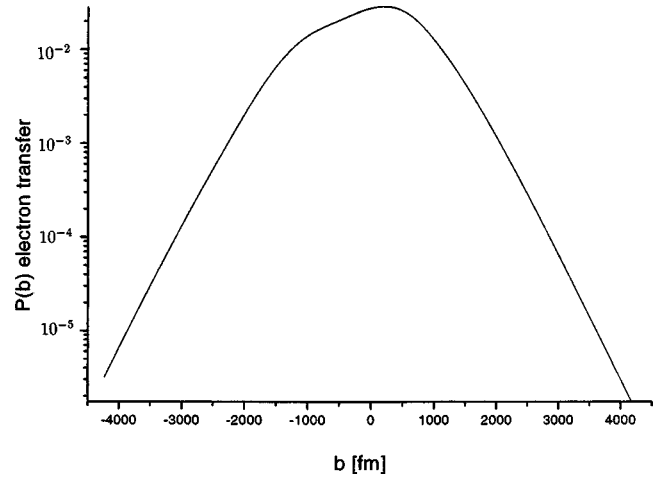

FIG. 4. Probability for transfer of the electron from the $1s_{1/2}(m_{j_x}=1/2)$ state of the target to the ground state of the projectile for the same collision system as in Fig. 2. The curve is calculated with the lattice method.

target is at rest in the right half of the figure at $(y=0,z=0)$, where noticeable density values indicate that the electron remains in the target state with a certain probability. The position of the projectile is that of the second maximum in the front left corner, which is an indication of the transfer process.

In Figs. 2–4 and in the following figures one recognizes an asymmetry of the probability distribution with respect to zero impact parameter. This behavior has the following origin. Depending on the sign of b the magnetic field of the
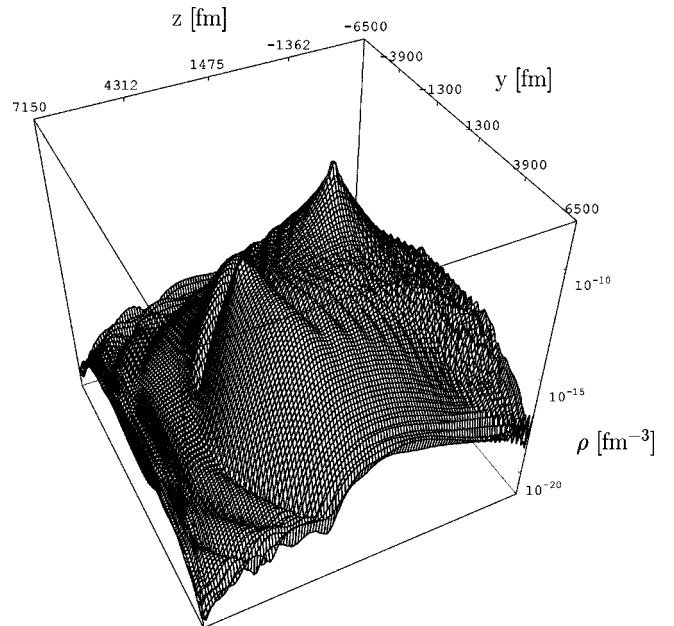

FIG. 5. Probability density of the time-developed electron state $1s_{1/2}(m_{j_x}=1/2)$ in the scattering plane in the collision of $U^{92+}(\gamma=1.5)$ on U^{91+} at the time $t=4780$ fm/c at an impact parameter $b=1060$ fm. The forward left peak is the transferred density around the projectile nucleus, the backward right peak is the remaining density around the target nucleus.

projectile has a different direction at the position of the target nucleus. Since the angular momentum of the initial $1s_{1/2}$ state is directed perpendicularly to the scattering plane, we have a different magnetic interaction for trajectories with a different sign of b and, therefore, we find slightly different probabilities. The same effects would result for a positive impact parameter and considering states with $m_{jx} = +1/2$ and $-1/2$.

B. Au^{79+}(930 MeV/nucleon)+U^{91+} scattering

To study the process of electron-positron pair creation with capture at low incident energies, we choose the scattering of Au^{72+} ions at 930 MeV/nucleon ($\gamma=2$) on U^{92+} ions. Experimental results of Belkacem *et al.* [3] as well as theoretical results are available. Momberger *et al.* [19] calculated probabilities for pair creation with capture by solving the Dirac equation in momentum space on a lattice.

We took a grid with 112 points in x direction (reflection symmetry is used) and 224 points in y and z directions. This grid has an extension from -6500 fm to 0 in the x direction and from -6500 fm to $+6500$ fm in the other directions. To get a better approximation between momentum and wave number, we now assume $n=2$ in relation (27). The time step is set to 25.4 fm/c. In order to obtain for the norm only a small deviation of less than 10^{-12} from unity, we expand the time-evolution operator up to the 25th order in the Hamiltonian. The wave function is evolved in time from $t= -5800$ to $+5800$ fm/c.

The probabilities for pair production with capture are obtained according to Eq. (12) by projecting the final wave function onto the states of the negative continuum of the target ion with quantum numbers $|\kappa| \leq 8$. For impact parameters $|b| \leq 60$ fm we use 448 energies for each κ ranging from $-8.8mc^2$ to $-mc^2$. For larger impact parameters already 224 states with energies from $-4.4mc^2$ to $-mc^2$ are sufficient.

Figure 6 shows the probability for pair production with capture of the electron into the U$^{91+}1s_{1/2}(m_{jx}=1/2)$ ground state. The full and dashed curves represent the results of the finite element treatment and of the perturbation theory, respectively. Since the upper limit of $t=5800$ fm/c is not sufficient for larger impact parameters, we assume perturbative values for $|b| \geq 800$ fm. At $b=0$ we can compare our value of 3.1×10^{-4} with the value of Momberger *et al.* who obtained 3.9×10^{-4} [19]. The cross section for pair production with capture results in $1.3b$ with the lattice calculation.

The distribution of the probabilities for pair production with capture are shown in Fig. 7 as functions of the κ values for special values of b. A rapid convergence in κ is reached for small impact parameters ($b=-58$ fm), but a very slow convergence for larger impact parameters ($|b|=530$ fm). The reason for the large contributions at high κ values is found in the occupation of bound states of the projectile by electron transfer. These bound states have negative energy parts in a basis of states centered around the target ion. The negative energy parts around the projectile could be incorrectly interpreted as positron contributions. As later explained in detail, we do not know the correct positron states for projecting on
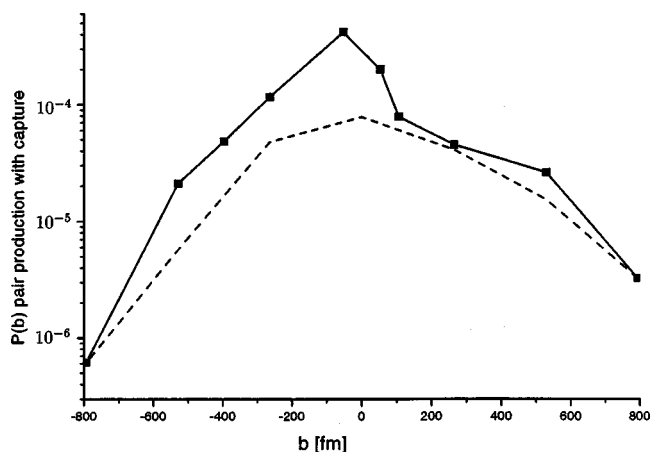

FIG. 6. Probability for electron-positron pair production with capture of the electron into the $1s_{1/2}(m_{j_x}=1/2)$ state of U^{91+} in the collision of Au$^{79+}(\gamma=2)$ on U^{92+} as a function of the impact parameter. The full-square points with $|b| < 800$ fm are calculated with the lattice method and connected with full lines. The dashed curve is the result of the perturbation calculation.

numerical wave functions. The correct positron states should also contain the contributions from the projectile ion, i.e., they have to be solutions of a time-dependent two-center Dirac problem. For instance, if we compare the differential probability of the positron states with $\kappa=-8$ and $m_{jx}=-4.5$, calculated by projection with our final wave function (full curve in Fig. 8), with the probability of the same states obtained by the projection on the boosted ground state of the Au^{78+} ion at $t=5800$ fm/c (dashed curve), we recognize an astonishing agreement. The dashed curve is adjusted in the way that the main maxima of both curves take the same height.

For a further insight in this problem, we calculated the density distribution generated by the states of the negative continuum contained in the time-developed wave function on the lattice. We projected our numerical solution for $b =530$ fm on the continuum states with $|\kappa| \leq 5$ and summed up all density contributions of the negative energy states. The resulting density distribution in the scattering plane is shown in Fig. 9. One clearly sees that the main part is located around the projectile and moves with the projectile.

A strong overlap of the boosted projectile ground state with the negative target continuum was already mentioned by Momberger *et al.* [19] for the same reaction. These authors found a probability of 0.018 contained in the negative continuum at $t=3680$ fm/c. With this value we can estimate the "false" contributions to the pair production which stem from the ground state of the projectile. We take the value 0.018 as the limit for $t \rightarrow \infty$ and multiply it with the cross section for charge transfer to the projectile which we determined to be $579b$ with our method. A further factor of 2 must be taken into account, because the cross section for charge transfer is averaged over both initial spin directions, whereas the cross section for pair creation includes the sum of both. This would lead to a cross section of pair creation with capture of $20.8b$, originating mainly from impact parameters larger than 2 reduced Compton wavelengths of the electron. This value is an unphysical result.
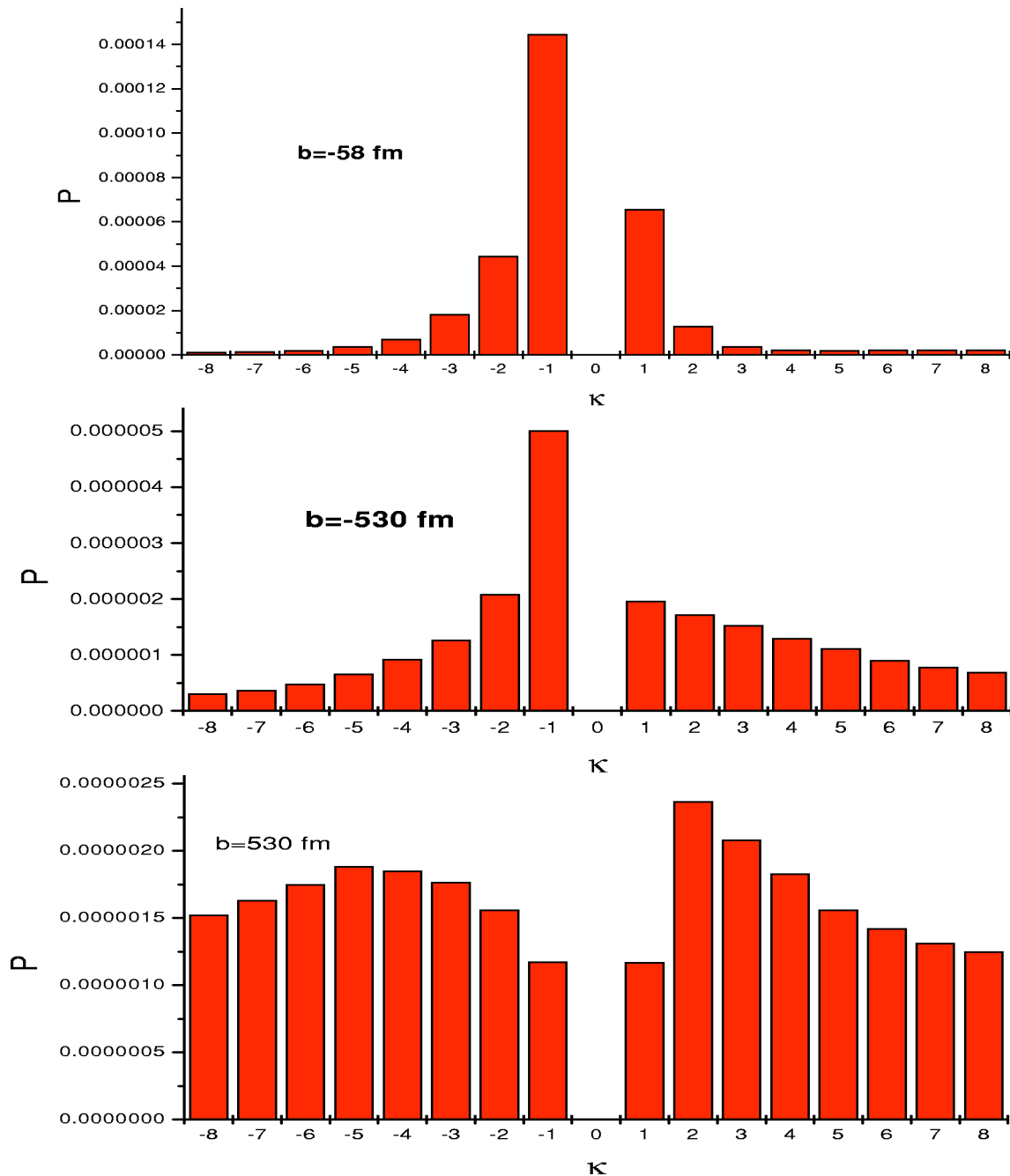
FIG. 7. Contributions to the probability for electron-positron pair production with capture of the electron into the $1s_{1/2}(m_{j_x}=1/2)$ state of U^{91+} in the collision of $Au^{79+}(\gamma=2)$ on U^{92+} for various κ values and the impact parameters $b=-58$, -530, and 530 fm.

The problems, discussed here, arise from the difficulty to define the positron states in a two center problem. Equations (10)–(12) assume that a positron is defined by a hole state in the negative continuum of the target ion after the collision. However, this definition is incorrect if a second ion, namely the projectile, is present independently of the distance. Instead of a projection with the target states of the negative continuum, in principle we must project with the time-dependent solutions of the Dirac equation with the electromagnetic potentials of two separating ions at very large distances $(t \to \infty)$. These solutions are two-center states perturbed around the ions, the use of which was already pro-

posed by Eichler [8] and Ionescu *et al.* [29], who faced the same problem regarding the process of pair creation with capture as a charge transfer process from the negative continuum of one of the ions to the bound states of the other ion.

In order to get rid of the contributions of the bound projectile ground state, we subtracted the contribution of this state from the wave function obtained on the grid. Therefore, we determined a complex amplitude for the impact parameter $b=530$ fm such that the spectrum in Fig. 8 nearly vanishes after having subtracted the contributions of the negative continuum inherent in the projectile ground state. Then we projected again on the negative continuum with
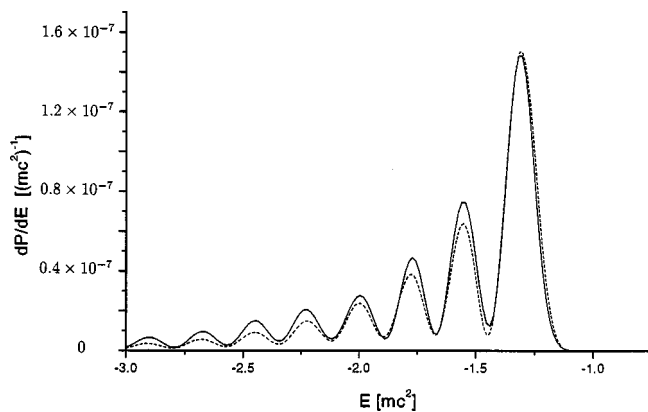
FIG. 8. Differential probabilities of the negative continuum states with $\kappa=-8$ and $m_{j_x}=-4.5$ in the lattice wave function (full curve) and in the wave function of the boosted projectile $1s_{1/2}(m_{j_x}=1/2)$ ground state of Au^{78+} (dashed curve). The latter probability is multiplied by a factor 3.1×10^{-3}. The impact parameter is $b=530$ fm.

states having different values of κ. The result is shown in Fig. 10, where the black boxes give the outcome of the corrected projection in contrast to the original results which are shown by grey boxes. The convergence in κ is now much better. Repeating this procedure also for other impact parameters, we finally obtain the cross section for pair production with capture into the target ground state of $1.1b$. If we estimate the contribution of captured electrons in higher shells by a factor of 1.2, valid for photon-induced pair production with capture in first order of αZ [30], there is still a gap to the experimental result of $2.19b$ [5].

The description of the system in terms of eigenstates of the target Hamiltonian becomes more adequate for higher projectile energies. At ultrarelativistic energies the transfer of the electron to the projectile is negligibly small and neither the electronic nor the positronic parts of the wave function can follow the projectile which travels nearly at the speed of light. The projectile potential is strongly Lorentz contracted and can be "turned off" after having passed the target region. Then the target basis alone is appropriate for the projection procedure.
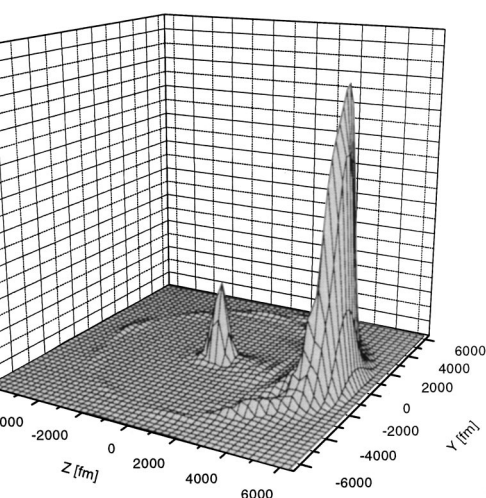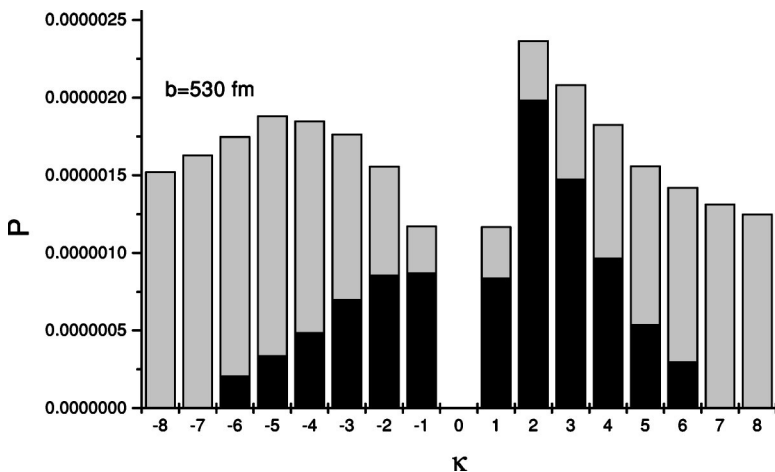

FIG. 9. Probability density of the negative continuum states in the scattering plane for the collision of $Au^{79+}(\gamma=2)$ on U^{92+} at $b=530$ fm. The projection has been done for angular momentum quantum numbers $|\kappa|\leq5$. The high maximum on the right-hand side arises due to the transferred electron and not due to the positrons.

C. Ultrarelativistic collisions of U^{92+} on U^{91+}

Here we consider the collision with a high value $\gamma_{FT}=10\,000$ of the Lorentz factor of the projectile for a fixed target. In order to avoid that the effective width of the Lorentz-contracted projectile potential becomes much smaller than the grid width, we start the calculation in the collider system where the target and projectile move with the same velocity v_c in opposite directions. Since the target and projectile systems are now contracted by the same Lorentz factor γ_c with respect to the collider system, we set the z range of our grid from $-z_0/\gamma_c$ to z_0/γ_c. Then the grid width is always small enough with respect to the extension and form of the electromagnetic potentials.

For $\gamma_{FT}=10\,000$ the Lorentz factor of the projectile and target in the collider system is $\gamma_c=((\gamma_{FT}+1)/2)^{1/2}=70.7$. We choose a lattice with 216 points in x and y directions ranging from -5000 fm to $+5000$ fm. In the z direction we take 324 points and set $z_0=7500$ fm. For the initial state we take the

FIG. 10. Probability for electron-positron pair production with capture of the electron into the $1s_{1/2}(m_{j_x}=1/2)$ state of U^{91+} in the collision of $Au^{79+}(\gamma=2)$ on U^{92+} at $b=530$ fm for various κ values. In the black boxes the parts are subtracted which originate from the electron transferred to the Au ion, the grey boxes have no subtractions. The grey boxes are the same as in Fig. 7.

TABLE I. Probabilities for the ground state and special excited bound states after the $U^{92+}(\gamma=10\,000)$ $+U^{91+}$ collision at $b=530$ fm.

State	Ultrarelativistic	This work	Perturbation theory
$1s_{1/2}(+1/2)$	0.524	0.528	
$2s_{1/2}(+1/2)$	4.565×10^{-2}	4.497×10^{-2}	8.628×10^{-2}
$2p_{1/2}(-1/2)$	9.329×10^{-4}	9.765×10^{-4}	1.848×10^{-3}
$2p_{3/2}(-1/2)$	5.049×10^{-3}	5.15×10^{-3}	1.169×10^{-2}
$2p_{3/2}(+3/2)$	7.049×10^{-3}	6.949×10^{-3}	1.609×10^{-2}

$1s_{1/2}$ solution of the von Mises iteration for a fixed nucleus and place it on the grid via a Lorentz boost. We start the calculation at $t_i=-2500/\gamma_c$ fm/c and end the time evolution at $t_f=2500/\gamma_c$ fm/c. The time steps are set to be $\Delta z/c$, so that both nuclei move the distance of the grid width Δz during this time. For the projectile potentials we again use the phase transformation given in Eqs. (49)–(51).

The minimum order of the expansion of the time-evolution operator, needed to keep the norm of the wave function constant, is about seven. This is much less than the one for low energetic collisions and is a hint that the process is more perturbative. The density of the final wave function differs only slightly from the density of the initial wave function, except for translation. This means that the transient projectile potential affects the wave function by a space-dependent phase factor only.

At the end of the time evolution we project on boosted target states. The expansion reads

$$\Psi(x,y,z,t) = \hat{S}\sum_n c_n \phi_n(x,y,\gamma_c(z-v_c t))$$
$$\times \exp(-iE_n \gamma_c(t-v_c z/c^2)/\hbar) \qquad (53)$$

with

$$\hat{S} = \cosh(\omega/2) + \sinh(\omega/2)\alpha_z, \quad \omega = \frac{1}{2}\ln\left(\frac{1+v_c/c}{1-v_c/c}\right),$$

where $\hat{S}$ is the boost matrix in z direction [1] and c_n are the expansion coefficients in the target system. Assuming that
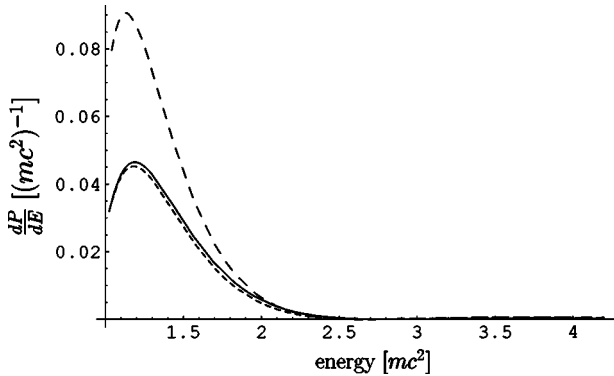
the effects of the projectile potentials on the wave function are negligible for $t \geq t_f$, we obtain the probabilities $P_n(t \geq t_f) = |c_n|^2$ in the target system.

For small impact parameters, a comparison of our work with the ultrarelativistic exact theory of Baltz [31] should be possible. The corresponding amplitudes are calculated by

$$a_f(t=\infty) = \langle \phi_f|(1-\alpha_z)\exp\left(i(E_f-E_i)\frac{z}{\hbar c}\right)$$
$$\times \exp(-i\alpha Z_P \ln\{[x^2+(y-b)^2]/b^2\})|\phi_i\rangle. \qquad (54)$$

In the following we give the results for an impact parameter $b=530$ fm. At first we examine the process of excitation of the target electron. In Table I we compare our results with those of the theory of Baltz [31] for infinite energies and with the results of the perturbation theory. Our results agree well with the ultrarelativistic limit, while those of the perturbation theory are about a factor of 2 too high.

In order to discuss the results for ionization and pair creation, we project the final wave function on $p_{1/2}$ states of the positive and negative continua with $m_{j_x}=-1/2$. Figure 11 shows the spectrum for ionization of the initially bound electron obtained with this method and compared with results of Baltz and from perturbation theory. Figure 12 gives the same quantities for the positron. In both cases the agreement of our results with the theory of Baltz [31] is very good whereas the perturbation theory tends to overestimate the nonperturbative results.

Thus we have numerically confirmed the ultrarelativistic theory of Baltz [31], using a quite different approach. By
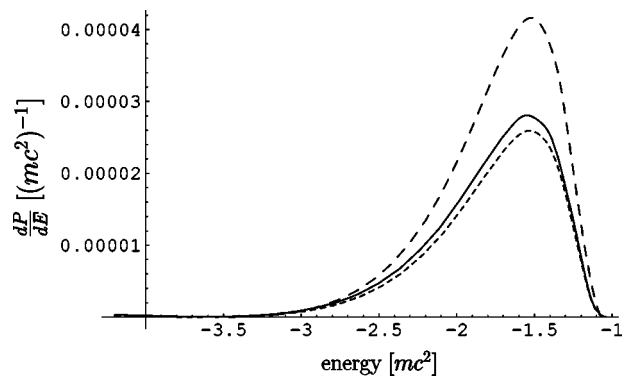

FIG. 11. Spectrum of emitted $p_{1/2}(m_{j_x}=-1/2)$ electrons at $b=530$ fm in the collision of $U^{92+}(\gamma=10\,000)$ on $U^{91+}(1s_{1/2})$. The full curve is obtained in the ultrarelativistic limit, the short-dashed curve with the numerical solution of the Dirac equation and the long-dashed curve with the perturbation theory.

FIG. 12. Spectrum of the $p_{1/2}(m_{j_x}=-1/2)$ positrons at $b=530$ fm in the collision of $U^{92+}(\gamma=10\,000)$ on U^{92+} The notation of the curves is the same as in Fig. 11.

switching to the collider system, this new method is useful to treat high Lorentz factors and does not need to make any approximations or assumptions about the structure of the electromagnetic potentials.

V. SUMMARY AND CONCLUSIONS

We have calculated probabilities for pair production with K-shell capture of the electron in the target by using the time-reversal symmetry method, where a $1s_{1/2}$ state of the target ion is developed in time under the influence of the electromagnetic fields of the projectile ion and finally projected on the positive and negative continua and bound states of the target. The time-dependent Dirac equation is numerically solved on a three-dimensional lattice in space with discrete time steps. These calculations simultaneously yield cross sections for the pair production with capture and the excitation, ionization and charge transfer of a K-shell electron.

For the collision system $U^{92+}(466 \text{ MeV/nucleon})+U^{91+}$ we reported on excitation, ionization, and charge transfer cross sections. The probabilities for these processes are found in good agreement with those of perturbation theory for larger impact parameters. For the case of the reaction $Au^{79+}(930 \text{ MeV/nucleon})+U^{91+}$ we calculated probabilities for pair production with K-shell capture by projecting on the negative continuum of target states. However, we found that these probabilities contain large parts stemming from the electron transferred to the ground state of the projectile. In order to get rid of these contributions, one must in principle introduce dynamical two-center states with the centers fixed at the target and the moving projectile. Here we simply subtracted the contributions of the negative continuum around the projectile which belongs to the transferred electron. The obtained cross section for pair production with capture is smaller than the experimental one. Our calculations show a moderate enhancement compared to the perturbation calculation, but the strong nonperturbative enhancement reported earlier [10] could not be seen.

The problems connected with the negative continuum states of the target are less important for higher collision energies. We made calculations for ultrarelativistic collision energies for the system $U^{92+}(\gamma=10\,000)+U^{91+}$ by applying a coordinate system in which both heavy ions have equal but opposite velocities. Our results agree with those of the exact theory of Baltz [31] for infinite collision energies.

[1] J. Eichler and W. E. Meyerhof, *Relativistic Atomic Collisions* (Academic, New York, 1995).

[2] H. Gould, Lawrence Berkeley Laboratory Report No. LBL-18593 UC-28, 1984.

[3] A. Belkacem, H. Gould, B. Feinberg, R. Bossingham, and W. E. Meyerhof, Phys. Rev. Lett. **71**, 1514 (1993).

[4] A. Belkacem, H. Gould, B. Feinberg, R. Bossingham, and W. E. Meyerhof, Phys. Rev. Lett. **73**, 2432 (1994).

[5] A. Belkacem, H. Gould, B. Feinberg, R. Bossingham, and W. E. Meyerhof, Phys. Rev. A **56**, 2806 (1997).

[6] A. Belkacem, N. Clayor, T. Dinneen, B. Feinberg, and H. Gould, Phys. Rev. A **58**, 1253 (1998).

[7] U. Becker, N. Grün, and W. Scheid, J. Phys. B **20**, 2075 (1987).

[8] J. Eichler, Phys. Rev. Lett. **75**, 3653 (1995).

[9] M. R. Strayer, C. Bottcher, V. E. Oberacker, and A. S. Umar, Phys. Rev. A **41**, 1399 (1990).

[10] K. Rumrich, K. Momberger, G. Soff, W. Greiner, N. Grün, and W. Scheid, Phys. Rev. Lett. **66**, 2613 (1991).

[11] M. Gail, N. Grün, and W. Scheid, J. Phys. B **36**, 1397 (2003).

[12] A. J. Baltz, M. J. Rhoades-Brown, and J. Weneser, Phys. Rev. A **44**, 5569 (1991).

[13] A. J. Baltz, M. J. Rhoades-Brown, and J. Weneser, Phys. Rev. A **50**, 4842 (1994).

[14] U. Becker, N. Grün, W. Scheid, and G. Soff, Phys. Rev. Lett. **56**, 2016 (1986).

[15] J. Thiel, A. Bunker, K. Momberger, N. Grün, and W. Scheid, Phys. Rev. A **46**, 2607 (1992).

[16] J. C. Wells, V. E. Oberacker, A. S. Umar, C. Bottcher, M. R. Strayer, J.-S. Wu, and G. Plunien, Phys. Rev. A **45**, 6296 (1992).

[17] J. C. Wells, V. E. Oberacker, M.R. Strayer, and A. S. Umar, Nucl. Instrum. Methods Phys. Res. B **99**, 293 (1995).

[18] J. C. Wells, V. E. Oberacker, M.R. Strayer, and A. S. Umar, Phys. Rev. A **53**, 1498 (1996).

[19] K. Momberger, A. Belkacem, and A. H. Sorensen, Phys. Rev. A **53**, 1605 (1996).

[20] D. Potter, *Computational Physics* (Wiley, New York, 1977).

[21] C. Müller, N. Grün, and W. Scheid, Phys. Lett. A **242**, 245 (1998).

[22] M. Abramowitz and I. A. Stegun, *Handbook of Mathematical Functions* (Dover, New York, 1972).

[23] O. Busic, Doctoral thesis, Universität Giessen, 2000.

[24] J. Eichler, Phys. Rev. A **35**, 3248 (1987); **37**, 287(E) (1988).

[25] J. C. Wells, B. Segev, and J. Eichler, Phys. Rev. A **59**, 346 (1999).

[26] C. Bottcher and M. R. Strayer, Ann. Phys. (N.Y.) **175**, 64 (1987).

[27] O. Busic, N. Grün, and W. Scheid, Phys. Lett. A **254**, 337 (1999).

[28] P. J. Mohr, G. Plunien, and G. Soff, Phys. Rep. **293**, 227 (1998).

[29] D. C. Ionescu and J. Eichler, Phys. Rev. A **54**, 4960 (1996).

[30] R. H. Pratt, Phys. Rev. **119**, 1619 (1960).

[31] A. J. Baltz, Phys. Rev. Lett. **78**, 1231 (1997).